RSC Advances

ROYAL SOCIETY OF CHEMISTRY

www.rsc.org/advances

Journal Name

ARTICLE

Formation of fluorescent platinum nanoclusters using hyper-branched polyethylenimine and their conjugation to antibody for bio-imaging

Received 00th January 20xx,
Accepted 00th January 20xx

DOI: 10.1039/x0xx00000x

www.rsc.org/

Xin Huang,[a] Hidekazu Ishitobi,[a, b] and Yasushi Inouye*[a, b, c]

We investigated the formation of yellow fluorescent polyethylenimine-protected platinum nanoclusters (Pt NCs@PEI) synthesized by a facile one-pot reduction method. Deep UV (DUV) Raman spectroscopy and attenuated total reflectance Fourier transform infrared (ATR-FTIR) spectroscopy were employed to estimate chemical bonding between Pt NCs and surrounding PEI ligands. We found that Pt NCs were procuced in the cavities formed by coiled PEI ligands and mostly stabilized with the amino groups ($-NH_2$). These Pt NCs@PEI with an average diameter of 1.4 ± 0.4 nm demonstrated excellent photo-stability against high salt concentration and long-term light exposure. By conjugating Pt NCs@PEI with the chemokine receptor anti-CXCR4 antibody, we successfully applied Pt NCs@PEI-(anti-CXCR4-Ab) conjugates to bio-imaging of the membrane of live HeLa cells that had their nuclei stained with DAPI. Moreover, Pt NCs@PEI showed lower cell cytotoxicity than Qdots@COOH, indicating they have better cell viability and great potential for bio-applications.

Introduction

Metal nanoclusters (M NCs) consisting of a few to several tens of atoms obtain size-dependent photoluminescence through the discretization of their electronic states.[1-3] The synthesis, characterization and application in fluorescence labelling of gold and silver nanoclusters (Au and Ag NCs, respectively) are widely studied.[4-10] On the other hand, while platinum nanoclusters (Pt NCs) are well established for their catalytic ability,[11-13] relatively little is known about their fluorescence capability and bio-imaging application as a fluorescent probe.

Some studies have reported the preparation of blue fluorescent Pt NCs using the surfactant-free method in N, N-dimethylformamide (DMF) solution[14] and yellow fluorescent Pt NCs protected with glutathione (GSH) using the ligand etching process.[15] We previously synthesized blue- and green-emitting fluorescent Pt NCs by using hydroxyl-terminated four generation poly(amidoamine) dendrimers (PAMAM(G4-OH)) as a template,[16, 17] finding the absolute quantum yield (QY) of the green-emitting Pt NCs to reach 28%. These fluorescent Pt NCs were applied to the labelling of chemokine receptors in living HeLa cells by binding them to an antibody *via* a conjugate protein. Additionally, multi-coloured fluorescent Pt NCs (from blue- to yellow-emitting fluorescence) were also prepared by utilizing hyper-branched polyethylenimine (PEI) as a stabilizer and employed for the quantitative detection of cobalt and copper ions with high sensitivity.[18]

In general, the stabilizing ligand or template (such as DNA, proteins, polymer, etc.) utilized in the synthesis of M NCs, plays a strong role in the effective prevention of NCs' irreversible coagulation and accurate tailoring of their size, dispersity, morphology, etc.[19] Recently, the interaction between M NCs and the surrounding ligand has drawn considerable interest in the NCs' formation process, transformation of the ligand, and origin of unique NCs' properties like fluorescence or catalysis.[20, 21] Several reports revealed that the embedment and formation of Au NCs inside the lysozyme or bovine serum (BSA) scaffold involve the changing of internal motion or configurational alternation of the ligand.[22, 23] Regarding the dendrimer template, Pt NCs have been formed by first complexing Pt^{2+} ions with PAMAM(G4-OH) mostly through amide(II) functional groups and then reducing the complex into Pt colloids.[24, 25] Interestingly, cationic polymer PEI, which is widely-used as a template to synthesize Au, Ag, and Pt nanomaterials,[26-29] has a prominent feature in that its chain conformation is strongly dependent on the medium pH: fully deprotonated (pH > 10), all primary amines protonated (pH □ 7), and most amines protonated (pH < 4).[30, 31] Luo et al. reported the synthesis of PEI-templated Ag NCs and assumed that a dense core caused by tightly coiled polymer chains could favour the stability of Ag NCs.[32] In contrast to the above studies, however, the formation of fluorescent Pt NCs in PEI ligands has not been illuminated in detail.

[a] *Graduate School of Frontier Biosciences, Osaka University, 1-3 Yamada-oka, Suita, Osaka 565-0871, Japan. Email: ya-inoue@ap.eng.osaka-u.ac.jp, TEL: +81-6-68794615; FAX: +81-6-68794619.*
[b] *Department of Applied Physics, Osaka University, 2-1 Yamada-oka, Suita, Osaka 565-0871, Japan.*
[c] *Photonics Advanced Research Center, Osaka University, 2-1 Yamada-oka, Suita, Osaka 565-0871, Japan.*

†Electronic Supplementary Information (ESI) available: Information about the experiment of conjugation Qdots to antibody, characterization about pH measurements, UV/Vis and photoluminescence spectrophotometric analysis, DLS and TEM measurements, quantum yield measurements, and supplementary Figures S1-S7. See DOI: 10.1039/x0xx00000x

In this paper, we investigated the formation process of Pt NCs in cationic polymer PEI ligands by employing Deep UV (DUV) Raman spectroscopy and attenuated total reflectance Fourier transform infrared (ATR-FTIR) spectroscopy to evaluate the chemical bonding between as-synthesized Pt NCs and surrounding polymer ligands. Then we characterized the aqueous yellow fluorescent PEI-protected Pt NCs (Pt NCs@PEI) by transmission electron microscopy (TEM), dynamic light scattering measurement (DLS), X-ray photoelectron spectroscopy (XPS), and spectrofluorometry. Furthermore, these Pt NCs@PEI were successfully applied to the bio-imaging of live HeLa cells upon effortless conjugation with an anti-chemokine receptor antibody, and the cytotoxicity of Pt NCs@PEI was also examined. Our investigation demonstrates the enormous potential of Pt NCs@PEI in the tracking, imaging, and labelling of cancer cells or other kinds of cells as an alternative to fluorescently-labelled probes.

Experimental

Materials

Hydrogen hexachloroplatinate (IV) hexahydrate ($H_2PtCl_6 \cdot 6H_2O$, 99.9%), sodium chloride (NaCl, 99.5%), hydrochloric acid (HCl, 0.1 M), rhodamine 6G, fluorescein, and 4', 6-diamidino-2-phenylindole (DAPI solution, 1 mg/mL in buffer) were purchased from Wako Pure Chemical Industries, Ltd. (Japan). Sodium borate buffer (SBB, pH = 9.0), COOH-functionalized CdTe QDots (QDots@COOH, λ_{em} = 570 nm), L-ascorbic acid (L-AA, 99.0%), and glutaraldehyde solution (50 wt.% in H_2O) were obtained from Sigma-Aldrich. Hyperbranched PEI (M_w = 10,000 g/mol, 99.0%) was purchased from Alfa Aesar (United Kingdom). N-hydroxysulfosuccinimide (Sulfo-NHS) and 1-(3-dimethylamino-propyl)-3-ethyl-carbodiimidehydrochloride (EDC, 98.0%) were obtained from Thermo Fisher Scientific Inc. (USA). APC anti-body-human CD184 (CXCR4) was purchased from Biolegend Inc. (USA) and human epithelial carcinoma HeLa cells were obtained from DS Pharma Biomedical Co., Ltd. (Japan). Phosphate buffered saline (PBS) tablets were purchased from Takara Bio Inc. (Japan). All experimental instruments used for synthesis were immersed in concentrated nitric acid solution and then copiously ultrasonically-washed by deionized water prior to use.

Characterization

Deep UV (DUV) Raman spectroscopy employed a 266 nm CW laser as the excitation light source and a laser intensity at the sample of 100 μW/μm^2. The exposure time for each spectrum was set to 15 or 60 s. A N.A. = 1.35 Ultrafluar objective lens (Glycerol immersion, Carl Zeiss) was used, and the transmitted light was guided into a spectrometer (SP2500, Acton Research) equipped with 1800 G/mm holographic grating. Raman spectra were measured using a cryogenically-cooled CCD camera (PyLoN, 2KBUV) at room temperature. Attenuated total reflectance Fourier transform infrared (ATR-FTIR) spectroscopy was acquired using ALPHA FTIR Spectrometer (Bruker Corporation, USA) with built-in diamond attenuated total reflection (ATR) optics. Interactive baseline correction of the ATR spectra was done using OPUS software (Bruker). X-ray photoelectron spectroscopy (XPS) was done using Kratos X-ray Photoelectron Spectrometer Axis Ultra DLD (Shimadzu Corporation, Japan). Confocal fluorescence imaging was performed with an FV1000 confocal laser scanning microscope (Olympus, Japan) using an oil immersion objective lens (40 ×, N.A. = 1.30), 473 nm excitation laser and appropriate emission filters.

Synthesis of Pt NCs@PEI

H_2PtCl_6 solution (80 μL) and aqueous PEI solution (400 μL, 15 mM) were added to 3 mL water solution under vigorous stirring to give a final H_2PtCl_6 concentration of 0.67 mM. After the complex formed under stirring for over 2 h, the mixture was heated to 95 °C and L-AA was added dropwise. The reaction was allowed to continue 2 days under vigorous stirring. The resultant Pt NCs were centrifuged by ultra-centrifugation (Optima MAX-XP Benchtop Ultracentrifuge, Beckman Coulter, Inc.; × 100,000 g) for 30 min at 4 °C twice. Subsequently, the NCs were dialyzed overnight using a dialyzer (cut-off molecule, 8000 g/mol) and centrifuged by a centrifugal filter unit (cut-off molecule, 3,000 and 10,000 g/mol) twice in order to remove unreacted small molecules.

Photo-stability measurement

The photo-stability of irradiated Pt NCs@PEI was measured as follows. Pt NCs@PEI, rhodamine 6G, and fluorescein were dissolved in sodium borate buffer solution. The samples were excited with 500 nm irradiation while the excitation bandwidth was set to 20 nm. The photo-stability of Pt NCs@PEI against salt was determined as follows. We mixed 300 μL of diluted fluorescent Pt NCs@PEI and 200 μL of each NaCl solution (0 to 1.0 M) to acquire a final concentration of Pt NC@PEI of 66.7 μM. After 30 min of mixing, the fluorescence properties were measured immediately three times using a fluorescence spectrophotometer.

Conjugation of Pt NCs@PEI to antibody.

A glutaraldehyde method was used to conjugate Pt NCs@PEI with antibodies.[33, 34] Pt NCs@PEI (3 μL, 66.7 μM in PBS) were diluted in 1 mL PBS solution containing glutaraldehyde (5% w/v) to a final concentration of 200 nM. The mixture was stirred under water bath with shaking at 37 °C. After 2 h, anti-CXCR4-Ab (20 μL, 1 mg/mL) was added to the mixture, which was then reacted for another 2 h. The whole mixture was allowed further incubation overnight at 4 °C. Lastly the Pt NCs@PEI-(anti-CXCR4-Ab) solution was centrifuged three times to remove any unreactive reagents and stored under 4 °C without light before use.

Cell culture and bio-imaging.

HeLa cells were cultured with Dulbecco's modified Eagle's medium (DMEM) in a 25 cm^2 tissue culture flask at 37 °C under a humidified atmosphere with 5% CO_2. The culture medium was replaced with freshly prepared medium once every two or three days. A culture dish containing HeLa cells was washed with PBS buffer, and new DMEM (500 μL) was added.

Then, Pt NCs@PEI-(anti-CXCR4-Ab) (50 nM, 150 μL) were introduced into the dish for 1 h at 37 °C. For nuclei staining, a culture dish containing HeLa cells was washed with PBS buffer and 2 mL DMEM was added. 150 μL DAPI (10 μg/mL) was introduced into the HeLa cells for 30 min at 37 °C, which were then washed with PBS followed by the addition of 500 μL DMEM and finally incubation with Pt NCs@PEI-(anti-CXCR4-Ab) (50 nM, 150 μL) for 1 h at 37 °C. Before observation, the cells were washed with PBS solution to remove any unbound reagents. Confocal fluorescence microscopy was employed to observe the HeLa cells.

Cell viability tests

Pt NCs@PEI- or Qdots@COOH-incubated HeLa cells (5.0 μL) at different concentrations were mixed with Trypan Blue (Invitrogen Japan K.K., 5.0 μL). 10 μL of samples were put on the chamber slide and then a Countess Automated Cell Counter (Invitrogen Japan K.K.) was employed to evaluate the cell viability. Each sample was measured three times in order to reduce the error.

Results and discussion

Chemical bonding between Pt NCs and PEI ligands.

Yellow fluorescent Pt NCs@PEI were prepared by a facile and environmental-friendly one-pot reduction method. Generally, polymer stabilizers were introduced to form a monolayer on the surface of the NCs to prevent agglomeration. Regardless of steric or electrostatic effects between the residual negatively charged NCs and the positively charged amines, interactions between the NCs and PEI were defined as weak covalent bonds.[35] In order to investigate the bonding information (i.e. binding sites) between Pt NCs and PEI, DUV Raman and ATR-FTIR spectroscopy were employed. Fig. 1a shows the DUV Raman spectra of pure PEI and Pt NCs@PEI. The bands appearing at 1450, 1307 and 792 cm^{-1} in pure PEI were assigned to CH_2 bending ($\delta(CH_2)$), wagging and rocking vibration of the methylene group ($\omega(CH_2)$ and $\rho(CH_2)$, respectively).[36, 37] Other bands at 1600 and 1080 cm^{-1} were attributed to amine bending ($\delta(NH_2)$) and amine stretching ($\upsilon(NC_3)$). After the reduction, the band at 1600 cm^{-1} remarkably decreased and shifted to 1560 cm^{-1} compared to pure PEI. We attributed this effect to a change in the protonation state of -NH_2 groups upon interaction with Pt NCs. Consistently, a shift in the -NH_2 bending mode to lower wavenumbers has been reported previously for PEI interacting with metal materials.[37, 38] Moreover, the band at 1450 cm^{-1} also slightly shifted (to 1430 cm^{-1}), which is another probable signature for bonding between PEI and Pt NCs.

As for the ATR-FTIR spectra (Fig. 1b), characteristic peaks of PEI were observed at 3349 and 3282 cm^{-1} (-NH, stretching), 2941 and 2821 cm^{-1} (-CH, asymmetric and symmetric stretching), 1632 and 1565 cm^{-1} (-NH, bending), 1465 cm^{-1} (-CH, bending), 1122 and 1040 cm^{-1} (-CN, stretching), which are all coincident with previous works.[39-42] Most characteristic peaks did not show obvious change after PEI stabilized with Pt NCs except for the wavenumber at 1632 cm^{-1}. The distinct change of this peak was possibly assigned to the approach of the primary amine to Pt NCs (Pt-ligand couple vibration mode).[24] A slight difference at 1346 cm^{-1} (-CH_2 wagging) was also an indication of bonding between the ligand and Pt NCs. Based on these spectroscopic results, we assumed that most Pt NCs were stabilized by the amino groups (-NH_2) of PEI rather than secondary or tertiary amines.

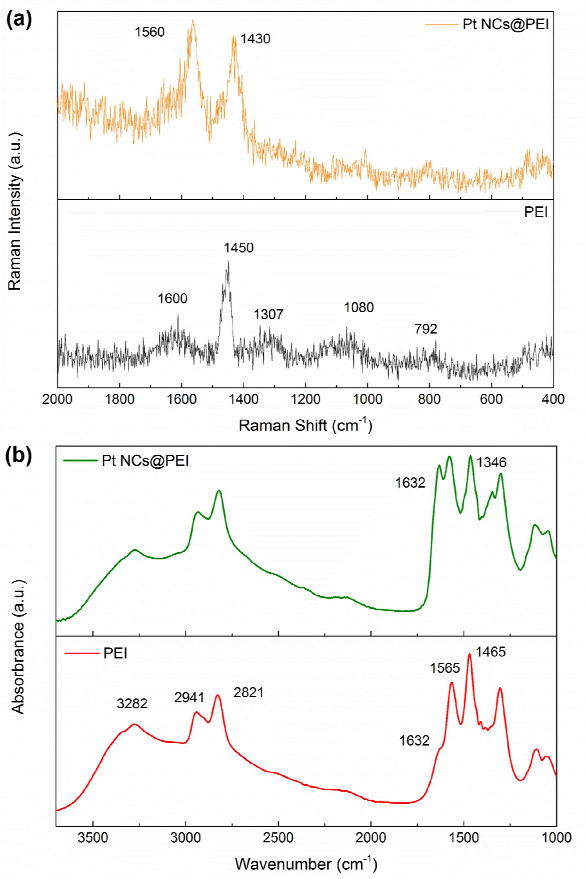

Fig. 1 (a) DUV Raman spectra and (b) ATR-FTIR spectra of pure PEI and as-synthesized Pt NCs@PEI.

Formation of Pt NCs in PEI ligand.

Investigation for the formation process of Pt NCs in the PEI template can facilitate understanding of the relationship between NCs and ligands. On basis of our spectroscopic results and previous studies,[32, 43] we described the formation of Pt NCs in the PEI ligand as two steps: First, the amino groups of PEI chelate with the Pt ions to form a complex (Scheme 1). This chelation corresponds to the interaction between Pt(IV) ions and PEI amines. The formation of the complex can be confirmed by a decrease in the absorbance of $[PtCl_6]^{2-}$ at 260 nm.[18] Second, L-AA reduces the Pt ions to Pt atoms for quick aggregation into Pt NCs inside a 'cavity' provided by tightly coiled PEI ligands. Instead of protonation, the high density of the amino groups can effectively chelate with Pt atoms when

the pH is basic, as this condition causes little or no electrostatic repulsion between PEI branches.[43] In this situation, the cavity could favour the protection of Pt NCs, and the size of the NCs is determined by the dimension of cavity. In addition, primary amine structures mostly appear around the cavities, offering stability to the Pt NCs, which is in agreement with DUV Raman and ATR-FTIR spectroscopic results.

Previously, significant pH-dependent variation in the fluorescent emission wavelength was observed during the synthetic process of Pt NCs.[18] Different from before, we fixed the molar ratio between Pt ions and reducing agent at 1:25 this time to synthesize the Pt NCs under various pH conditions (acidic, neutral, and basic). This pH-dependent emission wavelength is generated by the chain conformation of cationic polymer PEI. For the yellow fluorescent Pt NCs@PEI, the pH of the solution is basic. PEI could turn into fully deprotonated and have the ability to coil around the surface of Pt NCs to form the cavities (Scheme 1). As for the neutral condition (all primary amines protonated), the hydrodynamic size of Pt NCs is around 2.6 nm which is a little larger than ones produced under basic condition (close to 2 nm), resulting in the slight shift to 575 nm emission wavelength (Fig. S1 and S2). At acidic pH (most amines protonated), both PEI and PEI-capped NCs possess considerable positive charges, leading to an expansion of PEI chains because of the repulsion between the charged amines. The dimension of cavity in the acidic situation is much bigger than that in the basic situation, caused the larger Pt nanoparticles (NPs) and no emitted fluorescence. Judging from the size-dependent fluorescence properties of Pt NCs, the emission wavelength will shift to longer wavelengths under acidic conditions and shorter ones under basic conditions. Therefore, the size and fluorescent properties of Pt NCs@PEI is intensely related to the cavities formed by the coiled PEI ligands.

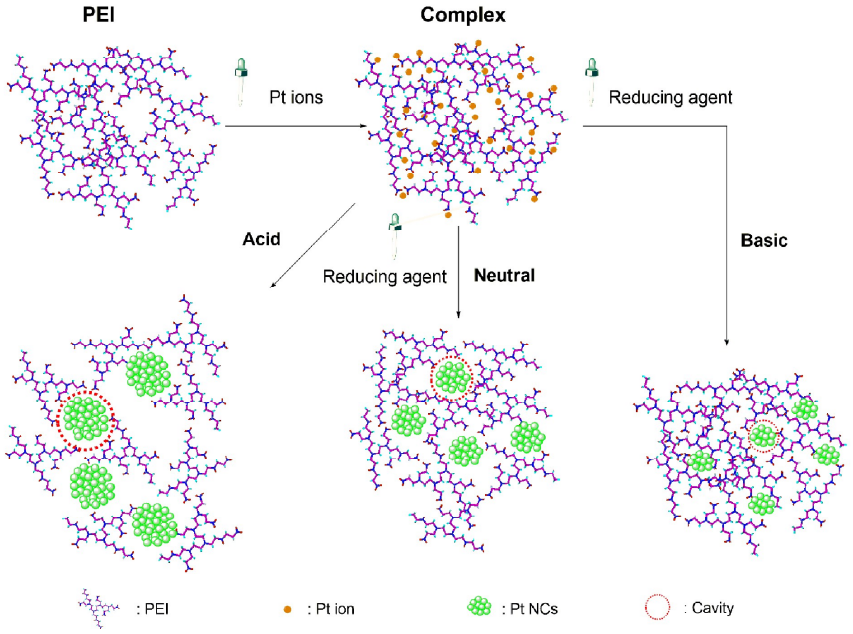

Scheme 1. Schematic formation of PEI chelation with Pt ions and reduced Pt NCs in PEI cavities at different pH mediums.

Physical characterization of Pt NCs@PEI.

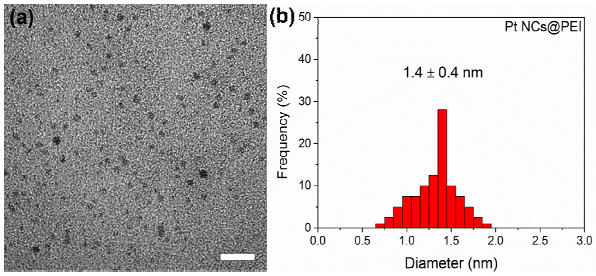

Fig. 2 (a) TEM micrograph of Pt NCs@PEI and (b) histograms of their size-distribution. Scale bar, 10 nm.

A typical TEM image of Pt NCs@PEI is shown in Fig. 2 and the average size of Pt NCs@PEI was 1.4 ± 0.4 nm. On the other hand, DLS results suggested the diameter to be closer to 2 nm (Fig. S1). This larger value is because DLS measurement provides the hydrodynamic size of Pt NCs@PEI.[5]

The oxidation state of Pt NCs@PEI was examined by XPS. The XPS spectrum of the Pt 4f region showed that $4f_{7/2}$ and $4f_{5/2}$ binding energies (B.E.) were 71.8 and 75.3 eV, respectively (Fig. 3). Since these values approximate the range of the Pt(0) state (71.3 - 72.4 eV), we concluded that Pt NCs@PEI were reduced to the zero valence. Comparatively, the $4f_{7/2}$ and $4f_{5/2}$ B.E. of pure bulk Pt were 71.4 and 74.9 eV, respectively (Fig. S3). A small positive-shift of B.E. between bulk Pt and Pt NCs@PEI indicated a charge transfer from Pt to N atoms of the amine ligand and a size effect of small NCs.[44, 45]

Furthermore, the 1s B.E. of N was 399.4 eV, which is a bit higher than that of typical N (398.4 eV), suggesting Pt NCs@PEI were stabilized by PEI ligands.

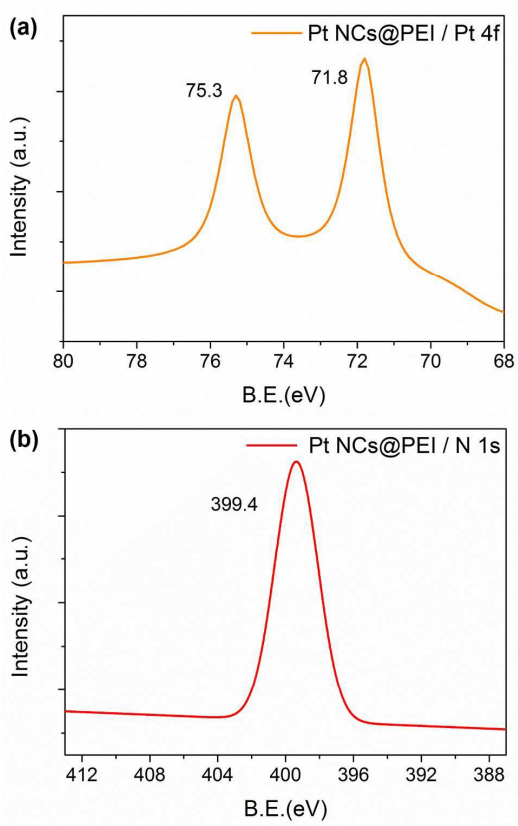

Fig. 3 XPS spectra of (a) Pt 4f and (b) N 1s regions of Pt NCs@PEI.

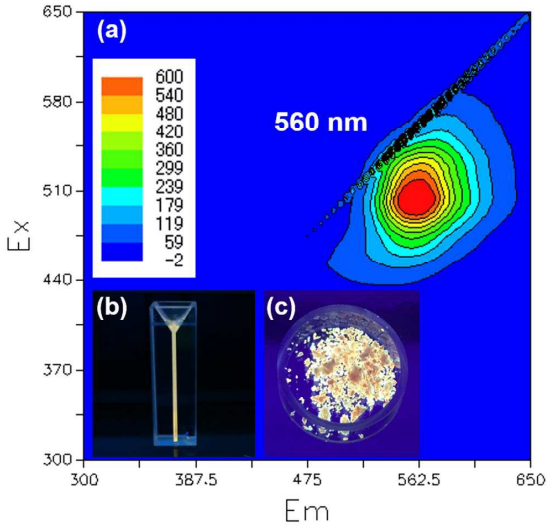

Fig. 4 (a) Excitation and emission matrix (EEM) spectrum of yellow-emitting Pt NCs@PEI. Insert are photographs of Pt NC@PEI in (b) solution state and (c) solid state.

Fig. 4a illustrates the excitation and emission matrix (EEM) spectrum of Pt NCs@PEI in aqueous solution. The maximum emission wavelength of Pt NCs@PEI was 560 nm when the excitation wavelength was 500 nm. Fig. 4b shows a photograph of yellow fluorescent Pt NCs@PEI in aqueous solution. It is noteworthy that the Pt NCs@PEI still emitted the yellow fluorescence even after drying to solid state (Fig. 4c). The relative QY of the Pt NCs@PEI was 6.8% using rhodamine 6G as a standard.

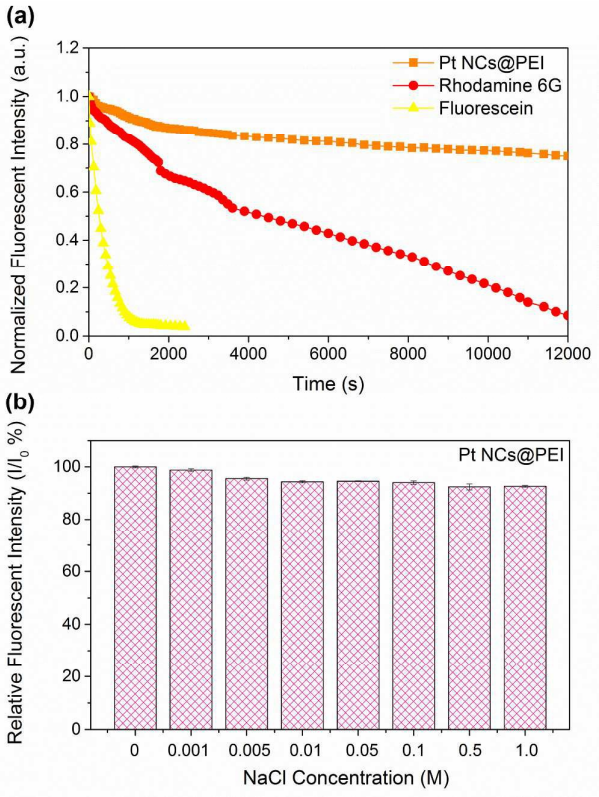

Fig. 5 (a) Fluorescence intensity of Pt NCs@PEI, rhodamine 6G, and fluorescein over time. (b) Histogram of Pt NCs@PEI' fluorescence (λ_{em} = 560 nm) in different NaCl solutions. The detection emission wavelength was 560 nm under 500 nm excitation wavelength.

The time-dependent variation in fluorescence intensity of Pt NCs@PEI was evaluated. Compared with two common organic dyes (rhodamine 6G and fluorescein), the fluorescence intensity of Pt NCs@PEI declined 20% after light irradiation for 12000 s while that of rhodamine 6G decreased 90% at the same condition (Fig. 5a). As for fluorescein, the fluorescence intensity practically vanished within 1000 s. Consequently, our Pt NCs@PEI possess superior photo-stability against photo-bleaching, which demonstrates significant advantage over organic dyes for single molecule detection and imaging. Photo-stability against chemical conditions is also crucial for bio-imaging and clinical applications. We examined the photo-stability of Pt NCs@PEI against salt concentration. Generally, citrate-stabilized metal nanoparticles (M NPs) have a poor

electrostatic stability resulting in aggregation when salt concentration exceeds 0.01 M. In contrast, we found the photo-stability of Pt NCs@PEI against NaCl concentrations up to 1.0 M to be relatively stable (Fig. 5b). The better tolerance against salt of Pt NCs@PEI than classically citrate-stabilized M NPs is because of the polymer ligand PEI, which prevents Pt NCs from aggregating in high salt concentration.

Bio-labelling of HeLa cells using Pt NCs@PEI.

In order to examine the bio-application of our yellow fluorescent Pt NCs@PEI, live cancer HeLa cells were employed as targets for bio-imaging. We bound Pt NCs@PEI to an anti-chemokine receptor antibody (anti-CXCR4-Ab) by using the common glutaraldehyde protocol to efficiently form Pt NCs@PEI-(anti-CXCR4-Ab) conjugates (Scheme 2). We compared emission spectra of the samples before and after conjugation with anti-CXCR4-Ab, finding negligible change in the fluorescence intensity and a consistent spectral shape (Fig. S4), which confirmed that Pt NCs@PEI-(anti-CXCR4-Ab) conjugates maintained fluorescence after conjugation.

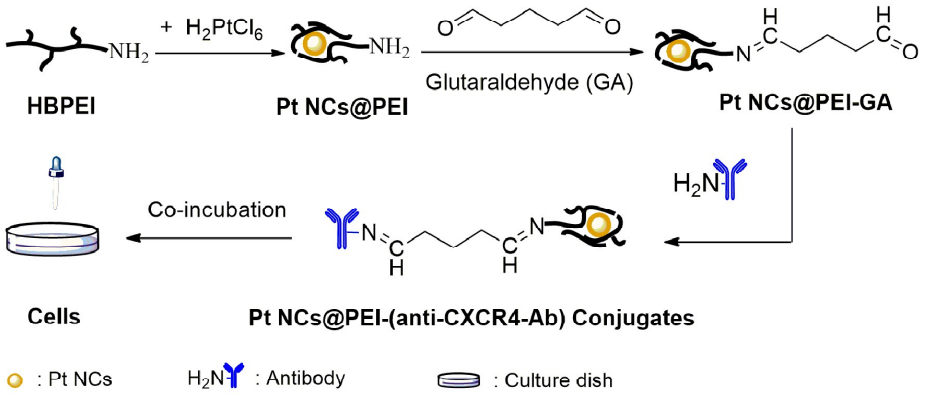

Scheme 2. Schematic reaction of the preparation of Pt NCs@PEI and bio-conjugation of Pt NCs@PEI to anti-CXCR4-Ab.

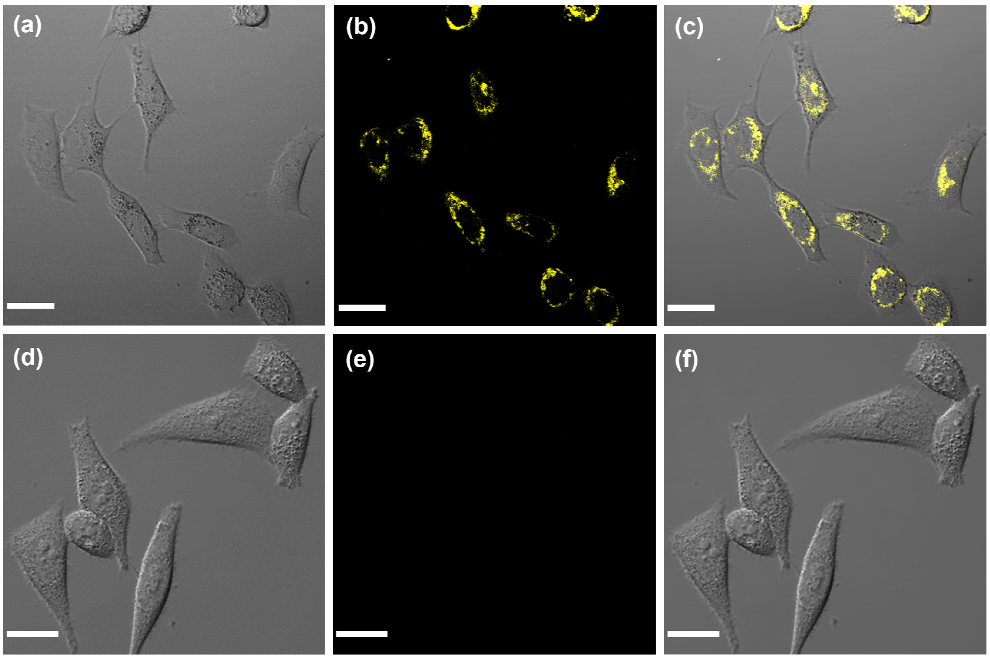

Fig. 6 Living HeLa cells labelled with Pt NCs@PEI-(anti-CXCR4-Ab) conjugates and imaged by (a) differential interference contrast (DIC) imaging and (b) laser confocal fluorescence microscopy. (c) The two images merged; Living HeLa cells not labelled with Pt NCs@PEI-(anti-CXCR4-Ab) conjugates and imaged by (d) DIC imaging and (e) laser confocal fluorescence microscopy. (f) The two images merged. Scale bars, 20 μm.

Pt NCs@PEI-(anti-CXCR4-Ab) conjugates were introduced into the cells and incubated for 1 h before confocal fluorescence microscopy imaging of the HeLa cells. Yellow fluorescence was clearly observed on the membrane of the HeLa cells, where chemokine receptors are expressed (Fig. 6). In order to examine the origin of the fluorescence, non-labelled HeLa cells were used as a control group. As expected, fluorescence from these cells was not observed, which indicates that the fluorescence was generated from the Pt NCs@PEI and not from auto-fluorescence of the HeLa cells.

DAPI was introduced to stain the nuclei of the HeLa cells to demonstrate the possibility of double staining with Pt NCs@PEI. Confocal fluorescence images show HeLa cell nuclei in blue (DAPI stained) and cell membranes as yellow, respectively (Fig. 7a, b). Fig. 7c, d shows double-staining images and demonstrates that the stained parts for DAPI and Pt NCs@PEI-(anti-CXCR4-Ab) conjugates were separated from each other due to the role of anti-CXCR4-Ab. These results confirm that the fluorescence signal of Pt NCs@PEI is not affected by other labels.

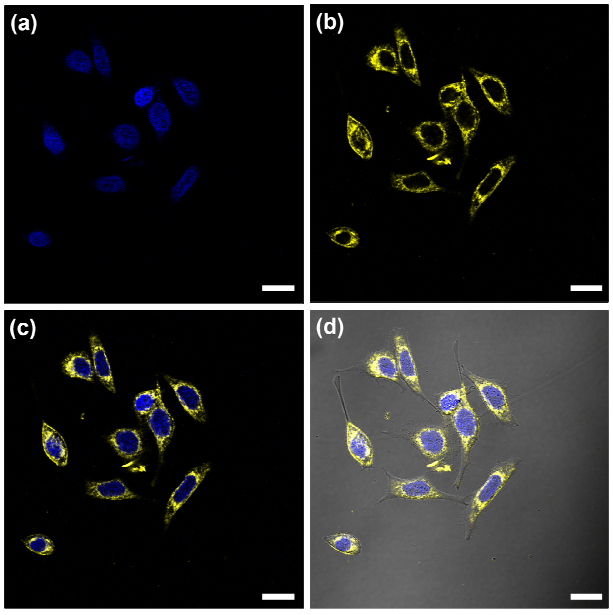

Fig. 7 Laser confocal fluorescence microscopic images of (a) Hela cells nuclei stained with DAPI and (b) the membrane labelled with Pt NCs@PEI-(anti-CXCR4-Ab) conjugates. (c) The merged image of (a) and (b). (d) Confocal fluorescence microscopy image merged with the differential interference contrast (DIC) image of double-stained HeLa cells. Scale bars, 20 μm.

The effect of the anti-CXCR4-Ab on the bio-imaging was also investigated. Anti-CXCR4-Ab can specifically bind to chemokine receptors that highly expressed in tumour cells.[46] The difference between the conjugation with and without this kind of antibody was determined by comparing Pt NCs@PEI and Pt NCs@PEI-(anti-CXCR4-Ab) conjugates as the targets under the same experimental conditions (concentration, incubation time, etc.). Regarding to the Pt NCs@PEI group, only little Pt NCs@PEI entered into the HeLa cells, as seen by the slight yellow fluorescence emitted (Fig. S5). On the other hand, more obvious yellow fluorescence was exhibited from cells when using Pt NCs@PEI-(anti-CXCR4-Ab) conjugates. Based on these results, we concluded that our Pt NCs@PEI could easily conjugate to bio-molecules in order to bio-label cancer cells and have the ability to achieve multi-color staining for cells without any interference from other fluorophores.

Cytotoxicity of Pt NCs@PEI

The cytotoxicity of a potential bio-marker must be considered for bio-imaging. Even if they have high QYs and tunable optical properties, high cytotoxicity may disqualify organic dyes or Qdots. The cytotoxicity for Qdots, for example, has been attributed to their release of toxic metal ions and the generation of reactive oxygen species (ROS).[47, 48] We evaluated the cytotoxicity of Pt NCs@PEI by comparing them with Qdots@COOH and a control group. No significant difference between cells treated with Pt NCs@PEI or the control group was found at 24 h (Fig. S6). At 48 h, the viability of cells treated with Pt NCs@PEI only decreased by ca. 10%, which agrees with our previous research.[16] This result demonstrates that Pt NCs@PEI have little acute toxicity and have potential for long-term study. In contrast, while the QDots@COOH group did not show remarkable cell damage within 1 h, weakening cell viability could be detected at 12 h, and cell activity was approximately halved by 24 h. At 48 h, the cell viability had dropped to ca. 33%. In addition, the effect of Pt NCs@PEI at different concentrations on cell viability was examined. Concentrations as high as 100 nM still caused little cytotoxicity, even at 48 h (Fig. S7). Thus, Pt NCs@PEI have lower cytotoxicity and better bio-compatibility than QDots@COOH.

Conclusions

The formation of fluorescent Pt NCs@PEI synthesized by a facile and environmental-friendly one-step reduction method was investigated. The forming of Pt NCs in PEI template was elucidated as two processes: 1) the chelation of PEI with Pt ions to form a complex and 2) the reduction of Pt ions to Pt atoms and the quick aggregation of these atoms to form Pt NCs, which were mostly stabilized *via* the amino groups (-NH_2) of PEI inside cavities produced by tightly coiled polymer chains. These ultra-small Pt NCs@PEI had a diameter of 1.4 nm and emitted bright yellow fluorescence at both solution and solid state. Furthermore, they demonstrated excellent photo-stability up to salt concentrations of 1 M and slower attenuation of fluorescence against long irradiation time compared with organic dyes. In addition, Pt NCs@PEI were easily conjugated with anti-CXCR4 antibody to produce Pt NCs@PEI-(anti-CXCR4-Ab) conjugates, which were successfully applied to

bio-imaging for the membrane of cancer HeLa cells whose nuclei were simultaneously stained with DAPI. These Pt NCs@PEI exhibited lower cell cytotoxicity and better bio-compatibility compared with Qdots@COOH, even at longer incubation times. The advantages of Pt NCs@PEI, such as water solubility, ultrafine size, and especially low cytotoxicity over common fluorophores (organic dyes and Qdots), suggest their potential as a safe and non-toxic fluorescent contrast agent.

Acknowledgements

One of the authors, Y. Inouye, gratefully acknowledges financial support from Grant-in-Aid for Scientific Research No. 24360026 and the Photonics Center, Osaka University, under the program of Photonics Advanced Research Center Program from the Ministry of Education, Culture, Sports, Science and Technology. The authors would like to thank P. Karagiannis for reading the manuscript.

Notes and references

1 J. Zheng, P. R. Nicovich and R. M. Dickson, *Annu. Rev. Phys. Chem.*, 2007, **58**, 409-431.
2 L. Shang, S. Dong and G. U. Nienhaus, *Nano Today*, 2011, **6**, 401-418.
3 I. Diez and R. H. A. Ras, *Nanoscale*, 2011, **3**, 1963-1970.
4 C. Sun, H. Yang, Y. Yuan, X. Tian, L. Wang, Y. Guo, L. Xu, J. Lei, N. Gao, G. J. Anderson, X.-J. Liang, C. Chen, Y. Zhao and G. Nie, *J. Am. Chem. Soc.*, 2011, **133**, 8617-8624.
5 X. Huang, Y. Luo, Z. Li, B. Li, H. Zhang, L. Li, I. Majeed, P. Zou and B. Tan, *J. Phys. Chem. C*, 2011, **115**, 16753-16763.
6 J. Wang, J. Ye, H. Jiang, S. Gao, W. Ge, Y. Chen, C. Liu, C. Amatore and X. Wang, *RSC Adv.*, 2014, **4**, 37790-37795.
7 C. Ding and Y. Tian, *Biosens. Bioelectron.*, 2015, **65**, 183-190.
8 J. Yu, S. Choi, C. I. Richards, Y. Antoku and R. M. Dickson, *Photochem. Photobiol.*, 2008, **84**, 1435-1439.
9 J. Li, X. Zhong, F. Cheng, J.-R. Zhang, L.-P. Jiang and J.-J. *Zhu, Anal. Chem.*, 2012, **84**, 4140-4146.
10 J. T. Petty, S. P. Story, J.-C. Hsiang and R. M. Dickson, *J. Phys. Chem. Lett.*, 2013, **4**, 1148-1155
11 K. Yamamoto, T. Imaoka, W.-J. Chun, O. Enoki, H. Katoh, M. Takenaga and A. Sonoi, *Nat. Chem.*, 2009, **1**, 397-402.
12 T. Imaoka, H. Kitazawa, W.-J. Chun, S. Omura, K. Albrecht and K. Yamamoto, *J. Am. Chem. Soc.*, 2013, **135**, 13089-13095.
13 T. Imaoka, H. Kitazawa, W.-J. Chun and K. Yamamoto, *Angew. Chem. Int. Ed.*, 2015, **54**, 9810-9815.
14 H. Kawasaki, H. Yamamoto, H. Fujimori, R. Arakawa, M. Inada and Y. Iwasaki, *Chem. Commun.*, 2010, **46**, 3759-3761.
15 X. Le Guével, V. Trouillet, C. Spies, G. Jung and M. Schneider, *J. Phys. Chem. C*, 2012, **116**, 6047-6051.
16 S.-I. Tanaka, J. Miyazaki, D. K. Tiwari, T. Jin and Y. Inouye, *Angew. Chem. Int. Ed.*, 2011, **50**, 431-435.
17 S.-I. Tanaka, K. Aoki, A. Muratsugu, H. Ishitobi, T. Jin and Y. Inouye, *Opt. Mater. Express*, 2013, **3**, 157-165.
18 X. Huang, K. Aoki, H. Ishitobi and Y. Inouye, *ChemPhysChem*, 2014, **15**, 642-646.
19 J. Li, J.-J. Zhu and K. Xu, *TrAC, Trends Anal. Chem*., 2014, **58**, 90-98.
20 Z. Wu and R. Jin, *Nano Lett.*, 2010, **10**, 2568-2573.
21 L. Su, T. Shu, J. Wang, Z. Zhang and X. Zhang, *J. Phys. Chem. C*, 2015, **119**, 12065-12070.
22 S. K. Mudedla, E. R. A. Singam, J. Vijay Sundar, M. N. Pedersen, N. A. Murugan, J. Kongsted, H. Ågren and V. Subramanian, *J. Phys. Chem. C*, 2015, **119**, 653-664.
23 X.-L. Cao, H.-W. Li, Y. Yue and Y. Wu, *Vib. Spectrosc.*, 2013, **65**, 186-192.
24 Y. Borodko, C. M. Thompson, W. Huang, H. B. Yildiz, H. Frei and G. A. Somorjai, *J. Phys. Chem. C*, 2011, **115**, 4757-4767.
25 Y. Borodko, P. Ercius, V. Pushkarev, C. Thompson and G. Somorjai, *J. Phys. Chem. Lett.*, 2012, **3**, 236-241.
26 H. Duan and S. Nie, *J. Am. Chem. Soc.*, 2007, **129**, 2412-2413.
27 T. Li, Y. Du and E. Wang, *Chem. Asian J.*, 2008, **3**, 1942-1948.
28 F. Qu, N. B. Li and H. Q. Luo, *Anal. Chem.*, 2012, **84**, 10373-10379.
29 F. S. Mohammed, S. R. Cole and C. L. Kitchens, *ACS Sustainable Chem. Eng.*, 2013, **1**, 826-832.
30 J. Nagaya, M. Homma, A. Tanioka and A. Minakata, *Biophys. Chem.*, 1996, **60**, 45-51.
31 M. Borkovec and G. J. M. Koper, *Macromolecules*, 1997, **30**, 2151-2158.
32 F. Qu, N. B. Li and H. Q. Luo, *Langmuir*, 2013, **29**, 1199-1205.
33 Z. Jie, Z. Jian, E. D. Allan and C. Y. Victor, *Nanotechnology*, 2013, **24**, 375102-37513.
34 H. Wu, H. Shi, H. Zhang, X. Wang, Y. Yang, C. Yu, C. Hao, J. Du, H. Hu and S. Yang, *Biomaterials*, 2014, **35**, 5369-5380.
35 D. V. Leff, L. Brandt and J. R. Heath, *Langmuir*, 1996, **12**, 4723-4730.
36 S. S. York, S. E. Boesch, R. A. Wheeler and R. Frech, *Macromolecules*, 2003, **36**, 7348-7351.
37 B. Chaufer, M. Rabiller-Baudry, A. Bouguen, J. P. Labbé and A. Quémerais, *Langmuir*, 2000, **16**, 1852-1860.
38 S. Sanchez-Cortes, R. M. Berenguel, A. Madejón and M. Pérez-Méndez, *Biomacromolecules*, 2002, **3**, 655-660.
39 W. Feng, K. C. Dev, L. Zhengquan, Z. Yong, F. Xianping and W. Minquan, *Nanotechnology*, 2006, **17**, 5786-5791.
40 O. Yemul and T. Imae, *Colloid Polym. Sci.*, 2008, **286**, 747-752.
41 F. Wang, P. Liu, T. Nie, H. Wei and Z. Cui, *Int. J. Mol. Sci.*, 2012, **14**, 17-29.
42 H. Cai, X. An, J. Cui, J. Li, S. Wen, K. Li, M. Shen, L. Zheng, G. Zhang and X. Shi, *ACS Appl. Mater. Interfaces*, 2013, **5**, 1722-1731.
43 F. Qu, N. B. Li and H. Q. Luo, *J. Phys. Chem. C*, 2013, **117**, 3548-3555.
44 T. T. P. Cheung, *Surf. Sci.*, 1984, **140**, 151-164.
45 C. Liu, G. Li, D. R. Kauffman, G. Pang and R. Jin, *J. Colloid Interface Sci*., 2014, **423**, 123-128.
46 A. Müller, B. Homey, H. Soto, N. Ge, D. Catron, M. E. Buchanan, T. McClanahan, E. Murphy, W. Yuan, S. N. Wagner, J. L. Barrera, A. Mohar, E. Verastegui and A. Zlotnik, *Nature*, 2001, **410**, 50-56.
47 J. Lovrić, S. J. Cho, F. M. Winnik and D. Maysinger, *Chem. Biol.*, 2005, **12**, 1227-1234.
48 Y. Su, M. Hu, C. Fan, Y. He, Q. Li, W. Li, L.-h. Wang, P. Shen and Q. Huang, *Biomaterials*, 2010, **31**, 4829-4834.

TOC:

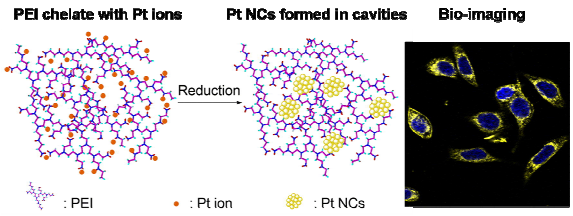

Fluorescent Pt NCs@PEI were formed in the cavities coiled by PEI ligands and bio-imaged HeLa cells *via* conjugation with antibody.